Optically Active Multilayer Films Based on Chitosan and an Azopolymer

ARTICLE *in* BIOMACROMOLECULES · FEBRUARY 2014

Impact Factor: 5.75 · DOI: 10.1021/bm500014r · Source: PubMed

5 AUTHORS, INCLUDING:

Raquel Fernández
University of Basque Country (UPV/EHU)
37 PUBLICATIONS **331** CITATIONS
SEE PROFILE

Susana C M Fernandes
KTH Royal Institute of Technology
44 PUBLICATIONS **597** CITATIONS
SEE PROFILE

Arantxa Eceiza
Universidad del País Vasco / Euskal Herriko U…
126 PUBLICATIONS **1,352** CITATIONS
SEE PROFILE

Agnieszka Tercjak
Universidad del País Vasco / Euskal Herriko U…
119 PUBLICATIONS **1,179** CITATIONS
SEE PROFILE

Article

pubs.acs.org/Biomac

Optically Active Multilayer Films Based on Chitosan and an Azopolymer

Raquel Fernández, Connie Ocando, Susana C. M. Fernandes, Arantxa Eceiza, and Agnieszka Tercjak*

Group 'Materials + Technologies' (GMT), Department of Chemical and Environmental Engineering, Polytechnic School, University of Basque Country (UPV/EHU), Plaza Europa 1, 20018 Donostia-San Sebastián, Spain

ABSTRACT: The layer-by-layer technique has been widely adopted for the fabrication of nanostructures with tailored properties. In this work, photoactive multilayer films consisting of alternating layers of chitosan and an azopolymer were developed by this method. Taking into account that pH is the factor controlling the charge of weak polyelectrolytes, the influence of this parameter on the structure and properties of the multilayer films was evaluated. Thus, different films were prepared by varying pH conditions as well as bilayer number. The morphology and properties of the films were analyzed by diverse advanced techniques, such as ultraviolet−visible spectroscopy, X-ray diffraction, and atomic force microscopy equipped with PeakForce QNM (Quantitative Nanomechanical Property Mapping). It was found that the thickness, roughness and elastic modulus of the developed multilayer films increased with the decrease of the chitosan solution pH and the increase of the bilayer number. Furthermore, induced birefringence measurements revealed that a higher level of photo-orientation was attained with the decrease of pH and the increase of bilayer number.

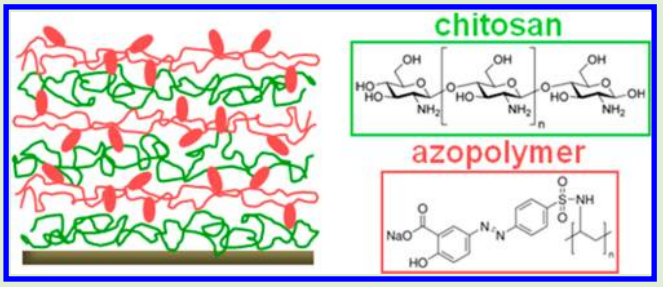

INTRODUCTION

During the past few years, there has been considerable interest in the development of nanostructured polymer films with controlled architecture and properties, as well as easy processability.[1] In this respect, layer-by-layer (LbL) adsorption of oppositely charged polyelectrolytes onto solid substrates has shown to be a versatile technique that does not require any sophisticated instrumentation and is independent of substrate shape, which is crucial for some applications.[1−3] Thus, polyelectrolyte multilayer (PEM) films can be built by electrostatic LbL self-assembly, where not only thickness and composition can be controlled precisely, but also their properties may be tuned synergistically with a combination of distinct materials in the same film.[1,4] The films obtained by LbL self-assembly are also very stable and robust, even in aqueous media, due to strong electrostatic interactions,[5] and have excellent adhesion to many substrates.[1] As a result, PEM films are useful for a variety of applications ranging from optical, electrochemical, and stimuli-responsive materials to biomedical devices and materials which mimic nature.[3,6] Indeed, the extraordinary precision with which PEM films are able to conform to even nanometer-sized pores and structures make these multilayer films exceptional for surface modification of a wide range of products and devices.[3]

Chitosan [(1 → 4)-2-amino-2-deoxy-β-D-glucan] is a polysaccharide derived from chitin [(1 → 4)-2-acetamido-2-deoxy-β-D-glucan], a natural polymer encountered in the exoskeleton of shrimps, crabs and other arthropods, as well as in the cell walls of fungi.[7] Whereas the applications of chitin are limited because of its poor solubility, chitosan, with a pK_a of around 6.5, behaves as a polycation in acid media and can be alternated with polyanions by the LbL technique.[8] In fact, chitosan is a biodegradable, biocompatible, nontoxic, and antibacterial biopolymer that has simple processing properties that make it a promising candidate for varied purposes, including food preservation and packaging, crop protection, cosmetics, and biomedical and pharmaceutical applications.[9,10] In this context, the fabrication of chitosan-based PEM films can be an interesting pathway to obtain high quality films in which properties can be manipulated or improved by combination with other compounds or polymers. For instance, Serizawa et al.[11] studied the coagulation of human blood on a LbL self-assembly of chitosan (procoagulant) and dextran sulfate (anticoagulant), showing alternating bioactivity on a polymer surface, as a function of the outermost layer of the film and the presence of sodium chloride. Chitosan has also been used to prepare PEM films with tunable drug delivery properties.[6] In particular, a drug delivery platform in hyaluronan/chitosan multilayer films was developed by Thierry et al.[12]

In addition to the advantages of these multilayer films, the LbL technique facilitates the incorporation of a wide variety of materials such as, for instance stimuli-responsive polymers, to develop PEM films in which some properties can be reversibly switched by an external stimulus.[13] Specifically, in combination with photoresponsive polyelectrolytes, light can be used to control PEM films properties, which is really attractive since the process generally does not produce additional chemicals and the reactions are typically clean and rapid.[2] Azobenzene and its

Received: January 5, 2014
Revised: February 24, 2014
Published: February 24, 2014

derivatives could be considered as excellent candidates for an optical molecular switch due to the reversible photoinduced isomerization between *trans* and *cis* isomeric states that these chromophores undergo upon exposure to light.[14] The formation of *cis* isomers leads to remarkable changes of size, dipole moment, and geometry of azobenzene molecules.[15] Consequently, polymers containing azobenzene groups or azopolymers have interesting photoresponsive properties, such as photoinduced chromophore orientation,[16−19] surface-relief-grating formation,[20,21] and photomechanical bending of thin films.[22−24] Therefore, the fabrication of PEM films containing azobenzene groups can be an efficient tool to control the properties of surfaces using light.[13] Examples of the interest in this research area can be found in various research investigations. Lim et al.[25,26] reported the fabrication of a photoswitchable multilayer film containing fluorinated azobenzene molecules that could be reversibly switched between superhydrophilicity and superhydrophobicity by irradiation with UV or visible light, respectively. Another example is the work of Goulet-Hanssens et al.[27] They reported the development of photoreversible cell culture substrates, composed of polyelectrolyte multilayers containing azobenzene groups, with different intrinsic capacities to support cell adhesion and survival upon light exposure.

In the present work, photoresponsive PEM films of chitosan, as the polycation, and a nontoxic water-soluble azopolymer consisting of a poly(vinyl amine) backbone with an azo dye as a side chain, as the polyanion, were developed and characterized by different advanced techniques. Atomic force microscopy (AFM) equipped with PeakForce QNM (Quantitative Nanomechanical Property Mapping) is a powerful tool for studying the local mechanical properties of materials and was used simultaneously to obtain the Young modulus and the topography of the multilayer films. In addition, PEM films fabrication is influenced by several variables, such as the use of weak or strong polyelectrolytes and the pH of the polyions solutions, among others.[28−32] Those parameters affect the structure and properties of PEM films and, therefore, were taken into account in the design of the optically active multilayer films.

EXPERIMENTAL SECTION

Materials. The azopolymer, poly[1-[4-(3-carboxy-4-hydroxyphenylazo)benzenesulfonamido]-1,2-ethanediyl, sodium salt] (PCBS), was supplied by Sigma-Aldrich and used as received. Medical-grade chitosan (CH) (degree of deacetylation of 96% and molecular weight of 300 000 g/mol, measured by viscosity) was purchased from Mahtani Chitosan PVT. Ltd. (India). CH was purified before use by a precipitation method.[33] Briefly, CH was dissolved in 1% (v/v) aqueous acetic acid solution, filtered, and precipitated by neutralizing with sodium hydroxide up to a pH = 8.5. The ensuing precipitate sample was washed with distilled water until a neutral pH and air-dried. The chemical structures of both materials are shown in Scheme 1.

Polyelectrolyte Multilayer Films Preparation. Films by LbL self-assembly of CH and PCBS were obtained. Aqueous solutions of both polyelectrolytes were prepared in concentrations of 5 g/L. The pH of PCBS solution in Milli-Q water was 9. In the case of CH, the pH of the solutions was adjusted within the range from 2 to 5 using hydrochloric acid and sodium hydroxide solutions. Washing solutions were Milli-Q water with the same pH as CH solution.

PEM films were deposited onto glass slides at room temperature. First, glass substrates were placed in a 'piranha' solution (70% sulfuric acid/30% hydrogen peroxide) for 30 min to clean and render a negative surface charge. The cleaned glass slides were then rinsed thoroughly with Milli-Q water and dipped alternately in the CH and PCBS solutions up to different number of layers, as represented in Scheme 2. In all cases, the last layer was of PCBS.

Scheme 1. Chemical Structures of (a) Chitosan and (b) PCBS

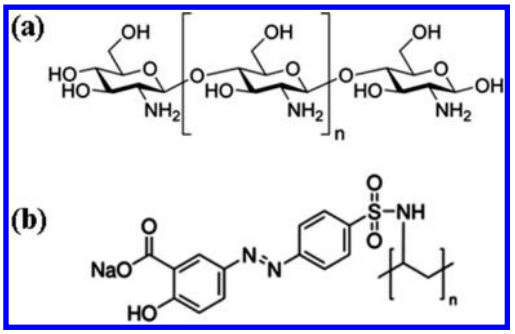

Scheme 2. Schematic Illustration of the Layer-by-Layer Process

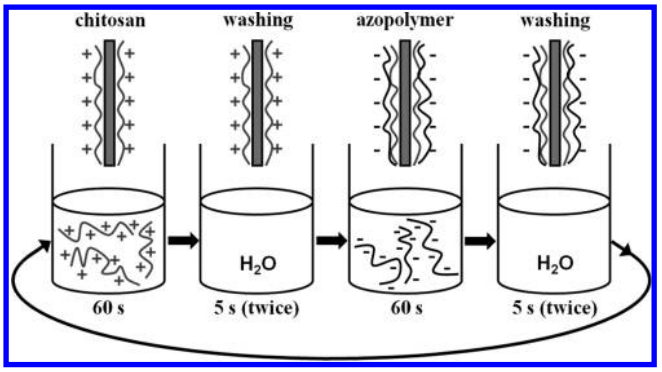

Polyelectrolyte Multilayer Films Characterization. *Ultraviolet−Visible Spectroscopy.* Ultraviolet−visible (UV−vis) absorption spectra of all PEM films deposited onto clean glass slides were recorded with a UV-3600 UV−vis−NIR spectrophotometer from Shimadzu.

Atomic Force Microscopy. The film thickness was determined by scratching the film partly off the glass slide surface and measuring the step height between the uncovered glass slide and the film by atomic force microscopy. AFM images were obtained with a Nanoscope IIIa scanning probe microscope (Multimode, Digital Instruments) under ambient conditions. Tapping mode in air was employed using an integrated tip/cantilever (125 μm in length with ca. 300 kHz resonant frequency and spring constant of ca. 40 N/m), with typical scan rates during recording of 0.7−1 line s^{-1}.

Morphological and quantitative nanomechanical properties of the developed PEM films were also investigated by AFM. In this case, measurements were performed using a Bruker Dimension Icon AFM operated under PeakForce mode in order to obtain high-resolution elastic modulus mapping under ambient conditions, with an integrated TAP150A tip having a resonance frequency of 142−162 kHz, spring constant of ca. 3.6 N/m and estimated tip radius of 40 nm.

X-ray Diffraction. X-ray diffraction (XRD) data were collected on a Bruker D8 Advance diffractometer equipped with a Cu tube, Ge(111) incident beam monochromator (λ = 1.5406 Å) and a Sol-X energy dispersive detector. The sample was mounted on a zero background silicon wafer embedded in a generic sample holder. Data were collected from 1 to 80° 2θ (step size =0.04 and time per step =353 s) at room temperature. A fixed divergence and antiscattering slit giving a constant volume of sample illumination were used.

Induced Birefringence Measurements. Birefringence was induced in PEM films under ambient conditions using a linearly polarized argon laser operating at 488 nm (pump beam) with a polarization angle of 45° with respect to the polarization direction of a low power

He−Ne laser operating at 632.8 nm (probe beam), as described elsewhere.[34] The power of the pump beam used in the experiments was varied between 6 and 20 mW on a spot of 0.4 mm^2, and the change in the transmission of the probe beam, which passed through the sample between two crossed polarizers, was measured with a photodiode.

RESULTS AND DISCUSSION

The polycation (CH) and the polyanion (PCBS) used to prepare photoactive multilayer films are weak polyelectrolytes. Consequently, the degree of ionization varied significantly with the change in pH, leading to variations in the thickness of the adsorbed material in the substrate. In order to study this effect, PEM films were fabricated under different pH conditions. Additionally, the number of chitosan/azopolymer bilayers was also modified.

Multilayer Films UV−Vis Absorbance. The UV−vis absorbance spectra of the different multilayer films as a function of the bilayer number and pH value are shown in Figure 1. An absorption maximum appears at around 365 nm, which corresponds to the electronic transition of azobenzene groups, responsible for the photoisomerization. As can be seen in Figure 1a, UV−vis absorbance increased almost linearly with the number of bilayers deposited, indicating a uniform absorption at each deposition step. Conversely, when increasing the pH (Figure 1b), the optical absorbance of PEM films decreased. Decher et al.[32] demonstrated that the thickness of PEM films could be fine-tuned at the molecular level through simple pH adjustments of the dipping solutions. This fact indicates that polyelectrolytes can change their conformation under different pH. In addition, the interactions between polyelectrolytes are also strongly pH dependent. In each chitosan/azopolymer bilayer interface, acid−base reactions between the carboxylic and amino groups take place, which result in proton transfer from CH to PCBS. The amino group in chitosan has a pK_a value of about 6.5, whereas PCBS contains a carboxylic acid for bonding which has a pK_a value of around 4−5. Here, the PCBS solution was maintained at pH = 9 and the CH solution was varied within the range of pH = 2−5. Thus, the azo-containing polyanion solution was at a high constant pH and, consequently, polymeric chains might have been completely charged and adopted an expanded conformation due to high electrostatic repulsions between polymer segments. Under lower pH conditions, less charged polymeric chains would adopt more globular conformations. In the case of the CH solution, when increasing the pH from 2 to 5, less polymeric segments became charged. In addition, it should be noted that pH not only controls the charge density of the adsorbing polymer, but also that of the previously adsorbed polymer layer.[30] When a PCBS chain is adsorbed onto a CH layer at a high pH (pH = 9), the degree of ionization of the chains in the solution is very high and in the deposition process they will interact with the CH chains in an attempt to neutralize the positively charged surface. If the pH of CH solution is very low (pH = 2), more polymeric segments will become charged and, hence, a higher amount of PCBS chains would be able to interact with the CH layer. On the contrary, if the pH of the CH solution is higher (pH = 5), less polymeric segments will become charged and lower amount of PCBS will be absorbed onto the previous CH layer. As depicted in Figure 1b, the maximum UV−vis absorbance was achieved for films fabricated under the lowest pH conditions (pH = 2). This result is in good agreement with the above assumption. At lower pH conditions, a higher amount of the photoactive polyanion was absorbed in the deposition process, leading to a higher UV−vis absorbance. The only exception occurred at pH = 3, a condition in which the films showed an absorbance lower than the expected. This fact was also observed by other authors.[8,35,36] A possible explanation for this behavior might be associated with a distinct coiling of the CH solution at pH = 3.[8]

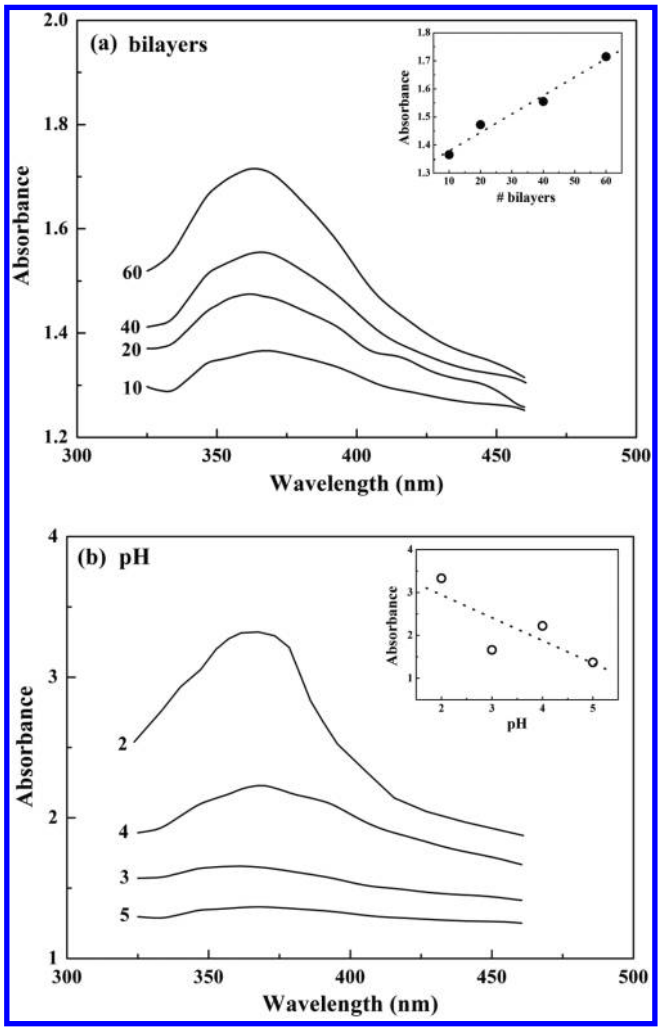

Figure 1. UV−vis spectra as a function of (a) bilayer number for PEM films obtained at pH = 5 and (b) pH for PEM films with 10 bilayers. The inner plots show the absorbance at 365 nm as a function of bilayer number and pH, respectively.

Multilayer Films Thickness. The thicknesses of the developed PEM films were also measured (Figure 2). For the same bilayer number, the films thickness decreased with increasing the pH (Figure 2a). Conversely, higher number of bilayers led to thicker films (Figure 2b). As rationalized above, the pH regulated the charge density of the CH as well as the amount of PCBS interacting with the CH. By increasing the pH, less charged CH chains might adopt more globular conformations, leading to thicker adsorbed layers; while, on the contrary, thinner adsorbed PCBS layers may be formed due to less possibility of ionic interactions with the CH layer. Based on the obtained results in Figure 2a, it could be stated that the effect of the pH, in the range of conditions evaluated, was greater on the thickness of the photoactive polyanion layer than on the CH layer thickness, giving rise to neat film thicknesses

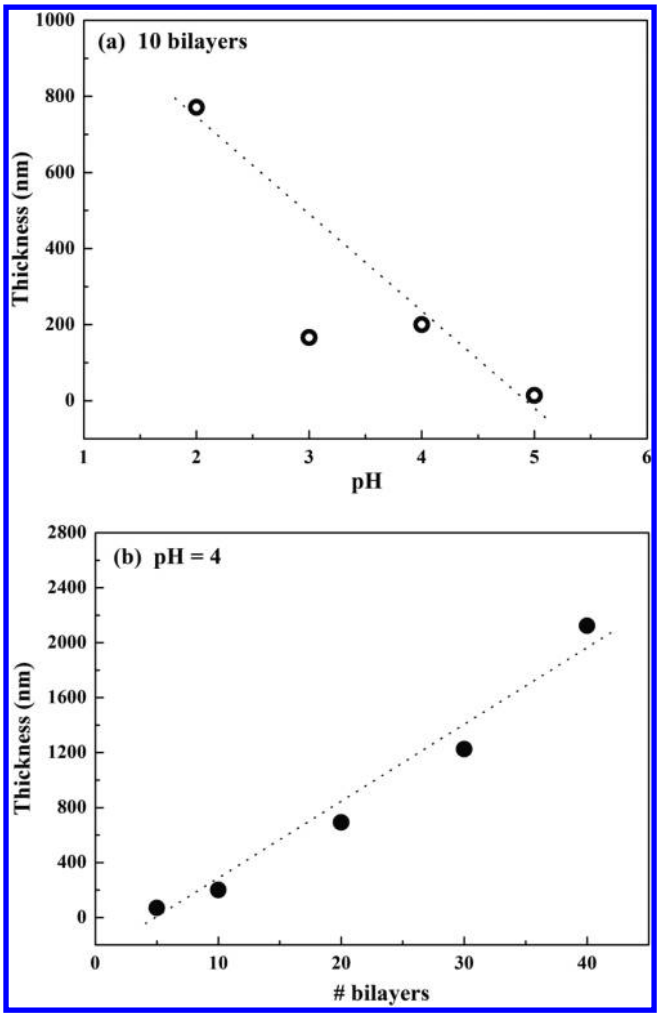

Figure 2. PEM films thickness as a function of (a) pH and (b) bilayer number.

higher with decreasing the pH of the CH solution. For pH = 3, a lower value of thickness than the expected was obtained, similar to the trend observed for the UV−vis absorbance of films. In fact, as was previously demonstrated,[30] dramatic changes in the thickness of sequentially adsorbed polyelectrolyte layers can be obtained with very small changes in the pH solution.

Multilayer Films Crystallinity. A study by X-ray diffraction was also carried out (Figure 3). Samples with different pH (3, 4, or 5) and the number of bilayers (5 or 20) were analyzed. Diffractograms indicate that PEM films present low crystallinity, which is characteristic for protonated CH.[35] Thus, in the LbL films, the CH was probably protonated because of the electrostatic interactions between adjacent layers.

Multilayer Films Morphology and Elastic Modulus. The variations of the pH and number of the bilayers can also have an influence on the PEM films surface morphology and properties. Indeed, it was demonstrated that multilayer films features have a great influence on some biological properties.[37] For instance, a major challenge in the field of tissue engineering is to optimize the surface characteristics to achieve a controlled level of cell adhesion under physiological conditions. Cell adhesion can be modulated through various surface properties, such as the topography[38] and stiffness[39] of the film, among others. In this paper, with the aim of analyzing the morphology

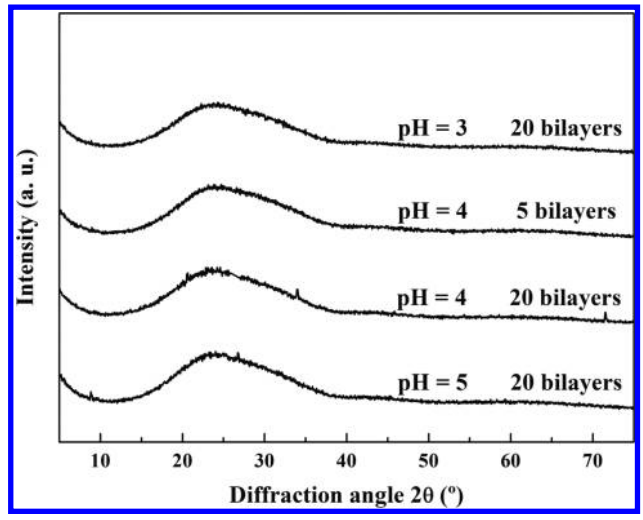

Figure 3. XRD spectra as a function of pH and bilayer number.

and mechanical properties of the obtained PEM films in depth, a study by AFM was performed. On the one hand, topographical images were obtained to investigate the surface morphology and roughness of the multilayer films. On the other hand, the nanomechanics of the developed PEM films were studied. Taking into account that AFM equipped with PeakForce QNM has emerged as a useful tool that allows quantitative nanomechanical mapping at high resolution of material properties, the Young modulus of the designed multilayer films was obtained by this advanced technique.[40]

Figure 4 shows topographic images of PEM films obtained by AFM. In order to achieve repeatable results, different areas of the samples were scanned. Since the roughness average (R_a) and the root-mean-square roughness (R_q) are the most widely used surface parameters, they were determined to analyze the roughness of the developed multilayer films. It was found that by increasing the pH, the PEM films roughness decreased (Figures 4a−c), but when increasing the number of bilayers, roughness increased (Figures 4c−e). As mentioned before, the pH has an effect on the charge density and conformation of the polyelectrolytes. In addition, the two oppositely charged polyelectrolytes might aggregate during the self-assembly process and this could lead to increase in the surface roughness together with an increase in the bilayer number.[41] Since the film thickness increased while decreasing the pH and increasing the bilayer number, in all cases, by increasing the thickness, the roughness increased. Fery et al.[42] also found that the surface roughness in multilayer films could be caused by changes in the salt concentration during the washing cycles. Upon water rinsing, salt ions which originally presented compensating charges in the PEM films are removed, thereby inducing structural rearrangements within the layers. As a result, also adjusting the salt concentration in this type of films, multilayers with controlled porosity can be achieved, which can find diverse applications.[42] In this work, washing solutions had the same pH as the CH solution.

The morphology of the multilayer films also changed as a function of the pH and the number of bilayers. By decreasing the pH and increasing the bilayer number, the number of surface bumps decreased and they became higher and wider. In general, this is in good agreement with the increase in roughness. The decrease in the number of surface bumps and the increase in their diameter might be related to a coalescence

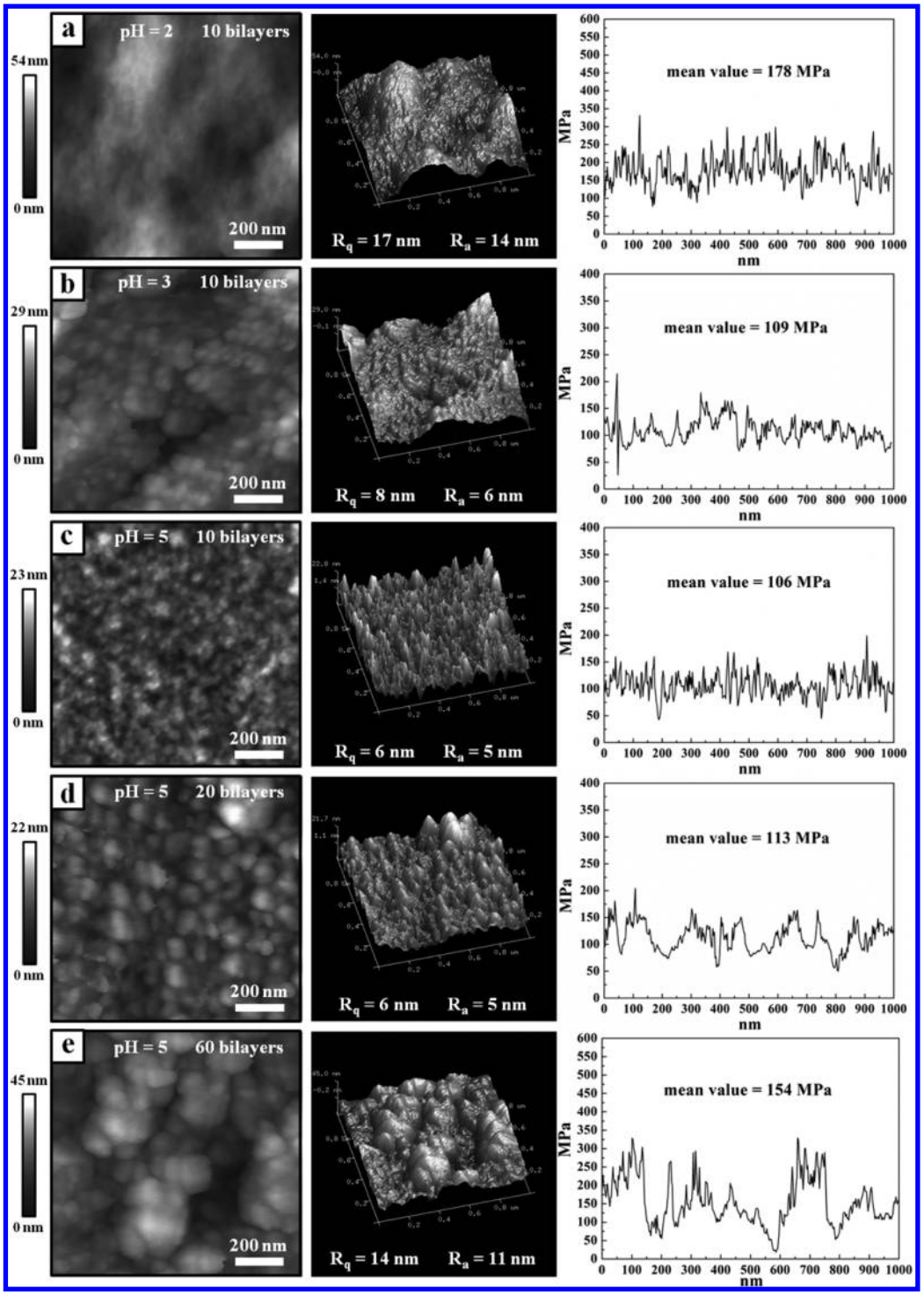

Figure 4. AFM topographic images (1 μm × 1 μm) and cross-section profiles obtained from PeakForce QNM of PEM films as a function of pH and bilayer number.

process and a consequent radial growth, due to the aggregation of smaller domains that merged into larger domains which were favored by electrostatic interactions. The increase of roughness during the coalescence process confirmed that surface bumps growth was also vertical.[43] Nevertheless, at pH = 5, the morphology of the sample with 10 bilayers was slightly different from that with 20 bilayers, even though both had similar roughness. The number and diameter of surface bumps changed, but not their height. This result would indicate that at pH = 5 the increase of bilayer number from 10 to 20 was not enough to induce a vertical growth of the surface bumps. In addition, as reported previously,[43] the orientation of the chromophores with respect to the glass substrate can be influenced by the surface morphology of the previous adsorbed layers. Specifically, it was demonstrated that at low roughness, PCBS chains were adsorbed with chromophores tilt orientated relatively to the substrate surface, since adsorption is mainly driven by electrostatic interactions. However, as the roughness increased, PCBS chains were also adsorbed on the bumps lateral surfaces, in such a way that an accumulation of J-

dx.doi.org/10.1021/bm500014r | *Biomacromolecules* 2014, 15, 1399−1407

aggregate "particles", aligned head-to-head, were adsorbed parallel to the substrate surface.[43]

Cross-section profiles of elastic modulus mapping images obtained from AFM of PEM films are also presented in Figure 4. The elastic modulus increased from around 106 to 178 MPa while decreasing the CH solution pH from 5 to 2 in PEM films of 10 bilayers; and from about 106 to 154 MPa as increasing the number of bilayers from 10 to 60 in PEM films obtained at pH = 5. Since the build-up of these multilayers results from the formation of interactions between the cationic and anionic groups of CH and PCBS, respectively; as a function of the pH, the number of ionized groups and interactions between layers might be different. This fact probably has an influence on the mechanical properties of PEM films, due to the differences in ionic cross-links between layers as a consequence of varying polyelectrolytes charge density.[44] The degree of ionization of the PCBS chains in solution is very high during all the deposition process since the pH is kept at a high constant value of 9. In the case of CH, by decreasing the pH solution its charge density increased. The increase in the charge density of the CH implies a higher amount of ionic interactions with the PCBS and a higher quantity of cross-links between layers. Assuming that the elastic modulus of the multilayer films is directly proportional to the density of ionic cross-links,[44] the modulus increased while decreasing the pH of the CH solution due to the increment of ionic interactions among layers. In addition, as mentioned above, the aggregation between polyelectrolytes increases with the bilayer number.[41] This effect might also have an influence on the Young modulus of PEM films, which increased when increasing the number of bilayers. Furthermore, it should also be noted that higher bilayer number and lower pH conditions could lead to higher amount of PCBS absorbed in the films. Consequently, the increase in elastic modulus might be also related to the increase in PCBS quantity in the multilayer films. In fact, the elastic modulus of a PCBS film obtained by dip-coating was also measured and resulted to be around 1 GPa, whereas the elastic modulus of a CH film is about 3 MPa. Cellular behavior is highly dependent on the modulus of the material. For instance, Sailer et al.[37] reported that human embryonic kidney cells (HEK 293) grow better in substrates with a higher modulus. Here we show that for the chitosan based multilayer films that were developed, the elastic modulus increased while decreasing the pH and increasing the bilayer number.

Multilayer Films Induced Birefringence. Our last goal was to investigate the optical properties of the designed PEM films containing an azopolymer. Azobenzene molecules can be oriented by irradiation with linearly polarized light of appropriate wavelength. Upon absorbing this light, azobenzene groups undergo a series of *trans*−*cis*−*trans* isomerization cycles. Those chromophores with dipole moment perpendicular to the polarization direction of the light electric field do not absorb light to undergo further isomerizations. At the end of several cycles, a net population of azobenzene molecules is oriented in this perpendicular direction, giving rise to a birefringence in the film structure. The birefringence formation can be inferred by the change in transmittance of a probe beam that passes through the sample between crossed polarizers. To investigate the kinetics of the chromophore orientation in the developed PEM films, the creation of the birefringence was followed over time through three different irradiation regimes (Figure 5): when the linearly polarized orienting beam was turned on (A), after it was turned off (B) and, finally, when irradiated with

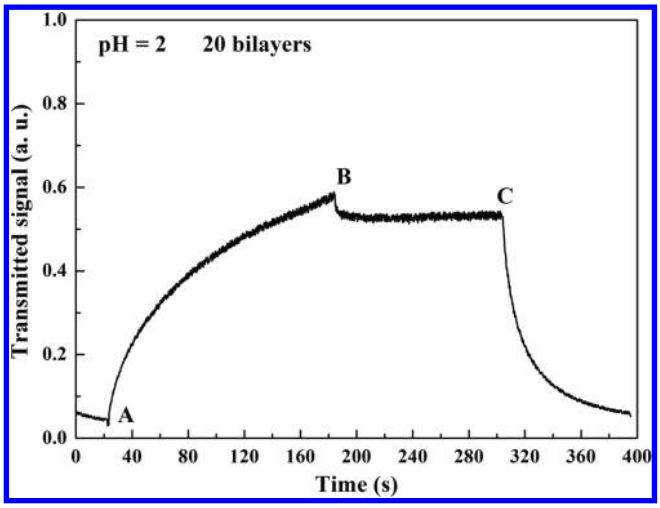

Figure 5. Induced birefringence and relaxation as a function of time at 6 mW of pump beam power for a PEM film of 20 bilayers obtained at pH = 2.

circularly polarized light to randomize the induced orientation (C). The transmitted signal was normalized between 0 and 1. At the beginning of the experiment there was no transmission of the probe beam, since the chromophores were randomly distributed. At point A, the pump beam was turned on, and the probe beam was transmitted through the polarizer-sample-polarizer system due to the birefringence induced in the film. When the pump beam was turned off at point B, molecular relaxation took place, but a considerable number of azobenzene molecules remained oriented, thus leading to a stable birefringence pattern. Finally, at point C, in order to remove the remaining birefringence, circularly polarized light was introduced, which completely randomized the induced chromophores orientation. This optical experiment was conducted with all the PEM films developed. However, for multilayer films obtained with pH = 5 the transmitted signal was too low to achieve clear plots, due to the low quantity of the PCBS adsorbed. Therefore, our investigation focused on the analysis of the optical behavior of the PEM films obtained with pH = 2, 3, and 4.

Figure 6 shows the maximum and remaining birefringence normalized with respect to the absorbance of films with 20 bilayers as a function of the pH. Both maximum and remaining values increased very significantly for the lowest pH employed (pH = 2). Generally, the capability of an azobenzene molecule to orientate depends on the irradiation wavelength, chromophore quantum yields, free volume available for the chromophores to orient, local environment around them, and polymer chain mobility; whereas the orientation relaxation when turning off the pump beam is only attributed to the free volume, the local environment around the chromophores, and the polymer chain mobility.[45] Thus, in order to develop a material with a maximal level of induced orientation, an equilibrium must be reached where the chromophores have enough freedom for isomerization and orientation, while also being in a polymer matrix that is stable enough that subsequent relaxation is minimized. As discussed above, lower pH conditions led to a higher amount of azopolymer absorbed in the deposition process. Since the transmitted signal is the result of the photoinduced orientation of the chromophores, a larger number of photoactive units in the films generated a higher birefringence and, thus, a higher signal transmission. In

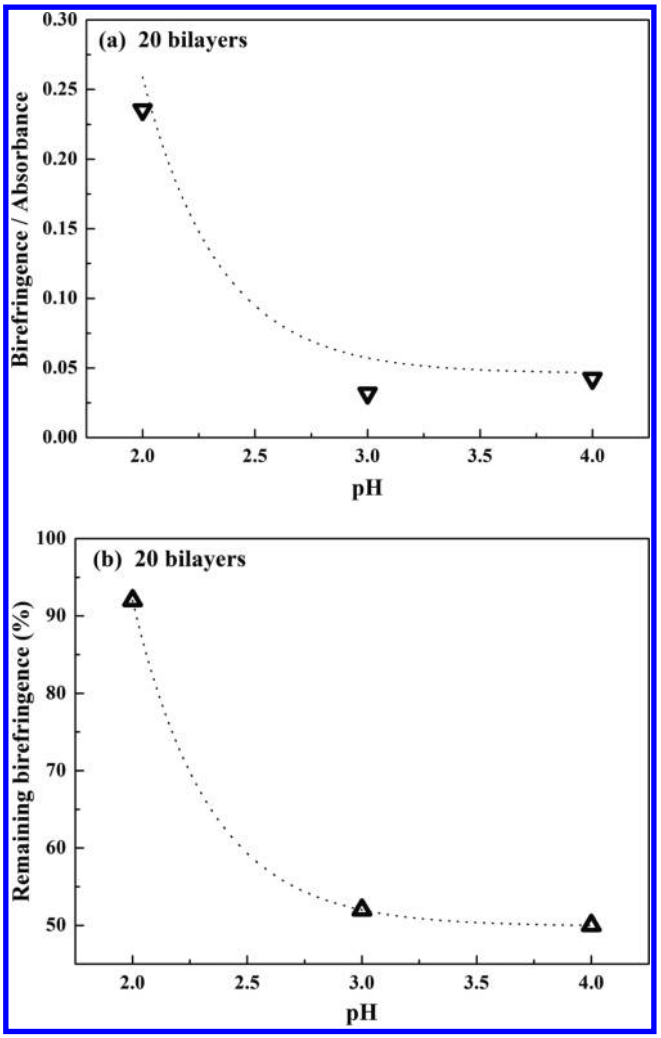

Figure 6. (a) Maximum birefringence and (b) remaining birefringence normalized with respect to the absorbance of PEM films with 20 bilayers as a function of pH.

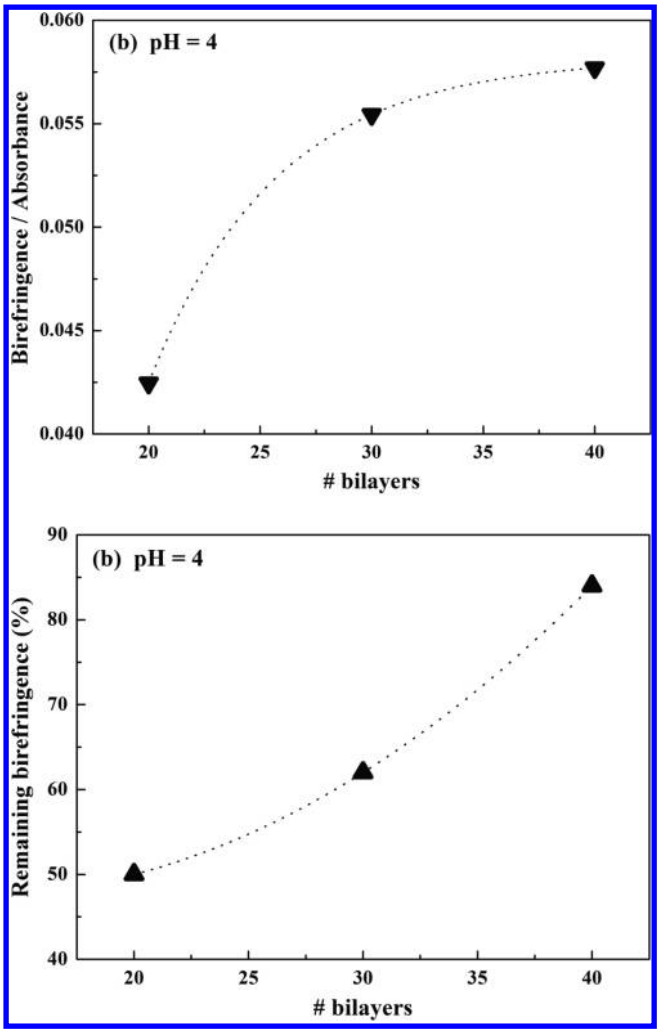

Figure 7. (a) Maximum birefringence and (b) remaining birefringence normalized with respect to the absorbance of PEM films obtained at pH = 4 as a function of bilayer number.

addition, the increase of cooperative interactions among azobenzene units, as a consequence of the increase in azopolymer concentration in PEM films at low pH, could also help to stabilize the induced orientation.[46] Indeed, the remaining photo-orientation for the PEM films obtained at pH = 2 was higher than 90%, while for multilayer films fabricated at pH = 3 and 4, around half of the induced orientation was lost after turning off the pump beam. Furthermore, as found by PeakForce quantitative nanomechanical mapping, the elastic modulus of the developed PEM films increased with the decrease in pH owing to higher number of ionic cross-links between layers. This fact might also contribute to the stabilization of the optically induced orientation. Certainly, it was demonstrated that dramatic changes in the properties of a sequentially adsorbed polyelectrolyte layer can be attained with very small changes in the pH solution.[30]

Conversely, when increasing the number of bilayers, both the maximum and remaining birefringence increased (Figure 7). A higher bilayer number implies an increase amount of azopolymer adsorbed, as well as higher cooperative interactions between azobenzene molecules. In addition, the study by AFM equipped with PeakForce QNM showed that the Young modulus of the PEM films increased with the bilayer number. These effects may contribute to the orientation creation and its stabilization.

The influence of the linearly polarized orienting beam power on the optical properties of the multilayer films was also evaluated (Figure 8). On the one side, the photo-orientation process was faster when increasing the power of the pump beam. At 6 mW of laser power, around 113 s were required to reach 80% of the maximum transmitted signal, while at 20 mW, 98 s were needed. As reported by Natansohn et al.,[47] the orientation rate is controlled by the photon flux, due to the statistical nature of the process. The more photons the sample absorbed, the more possible photo-orientations. In addition, the level of the transmitted signal increased with the number of photons involved in the orientation process. This could be due to the fact that, as the laser power increased, a thermal effect took place and the heat from the irradiation of the pump beam was enough to increase the temperature around the irradiating point. This sample heating might induce greater chromophore mobility, leading to a faster process and a higher level of photo-orientation. However, on the other side, the remaining transmitted signal decreased from about 90% to around 80% when increasing the pump beam power from 6 to 20 mW. In this case, the thermal effect probably caused the higher chromophore mobility to relax, counteracting the orientation

dx.doi.org/10.1021/bm500014r | Biomacromolecules 2014, 15, 1399−1407

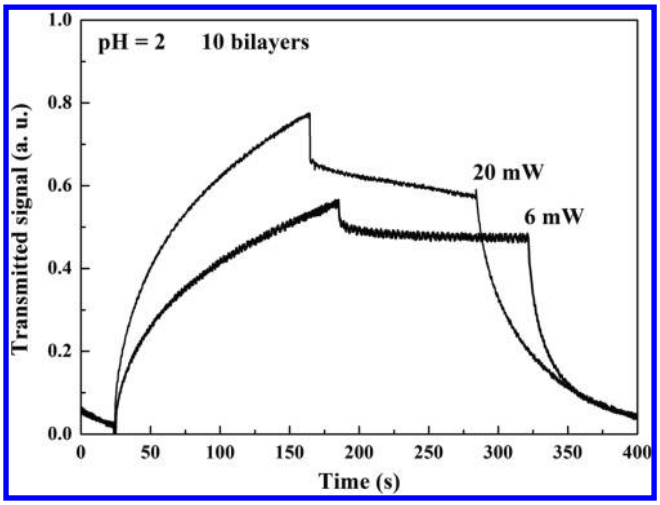

Figure 8. Induced birefringence and relaxation as a function of time at two different pump beam powers (6 and 20 mW) for a PEM film of 10 bilayers obtained at pH = 2.

stabilization. The same kind of results as a function of laser power was obtained for the rest of the PEM films fabricated.

Up to this point, in all cases, results of the analysis of the first orientation-relaxation cycles of around 3 min long were shown. Additionally, successive orientation-relaxation sequences, as represented in Figure 9a, were investigated. After successive cycles, a higher level of orientation was attained. It was verified that saturation level was reached after around seven orientation-relaxation cycles. In general, the photo-orientation process in PEM films is considerably slower than in spin-coated or cast films because the electrostatic interactions in these multilayer films cause the chromophores to be more densely packed, with lower mobility, hindering molecular alignment.[48] Additionally, a first cycle was performed up to the saturation level (Figure 9b). As a result of the slow rate of the chromophores orientation due to electrostatic interactions, at least 1 h was needed to reach a well-defined steady state. With regard to the remaining transmitted signal, its value kept approximately constant in all performed cycles.

CONCLUSIONS

Photoactive multilayer films consisting of alternating layers of chitosan and an azobenzene-containing polymer were fabricated and characterized. In order to tune electrostatic interactions, the pH of the CH solution was varied. As a result, the designed PEM films UV−vis absorbance and thickness increased with decreasing the pH, owing to a greater possibility of the PCBS to interact with the charged CH layer, giving rise to a higher amount of adsorbed azopolymer. Multilayer films UV−vis absorbance and thickness also increased with increasing the bilayer number.

AFM images indicated that the surface roughness of the developed PEM films was at nanometer scale and increased with the bilayer number due to aggregation as well as by decreasing the CH solution pH. The elastic modulus, obtained by PeakForce quantitative nanomechanical mapping, also increased with the bilayer number and with the decrease in pH. The pH decrease produced an increase in the CH charge density, which led to a higher amount of cross-links with the PCBS that contributed to the modulus increase.

The optical response of the developed PEM films was also investigated. The induced photo-orientation was higher when

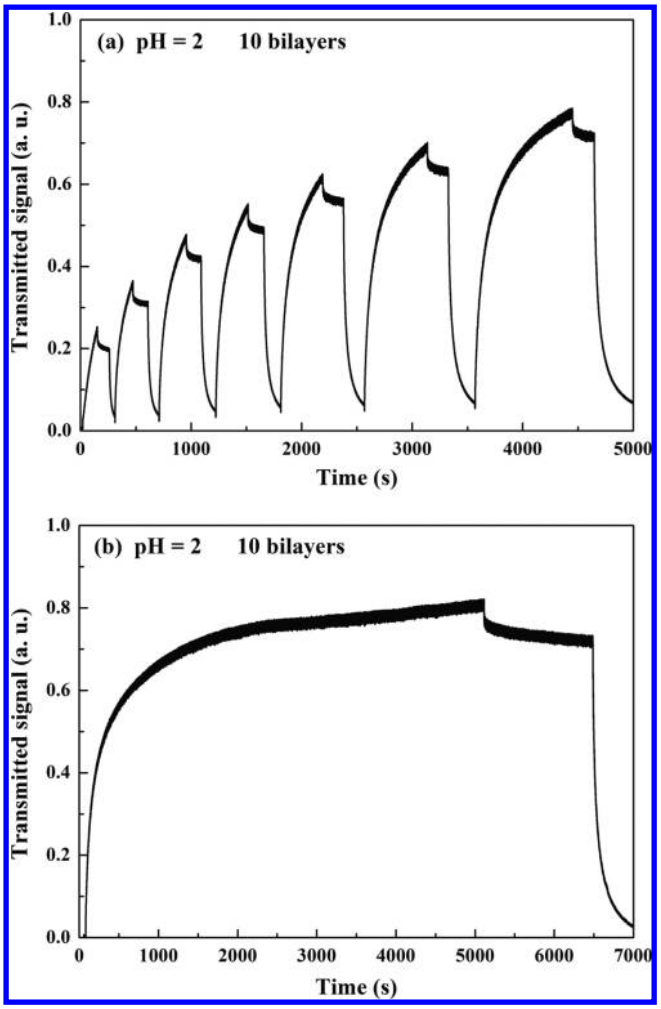

Figure 9. (a) Successive cycles and (b) long cycle until saturation of induced birefringence and relaxation as a function of time at 6 mW of pump beam power for a PEM film of 10 bilayers obtained at pH = 2.

decreasing the pH and increasing the bilayer number, mainly due to a larger concentration of photoactive azobenzene groups in the films and cooperative effects among them.

Finally, it is worth mentioning that this kind of optically active multilayer films could find applications in diverse biotechnological areas and can be adapted to the requirements of each sector. Our future studies will include biocompatibility tests with cells.

AUTHOR INFORMATION

Corresponding Author

*Tel.: +34 943 017 163; fax: +34 943 017 130. E-mail address: agnieszka.tercjaks@ehu.es.

Notes

The authors declare no competing financial interest.

ACKNOWLEDGMENTS

Financial support from the Basque Government (Grupos Consolidados (IT776-13) and SAIOTEK2013 (NANOSOL)) and from the Spanish Ministry of Economy and Competitiveness (MINECO) (MAT2012-31675) is gratefully acknowledged. We also wish to acknowledge the 'Macrobehaviour-Mesostructure-Nanotechnology' SGIker unit and Aitor Larrañaga, from the 'Molecules and Materials' SGIker unit, for

performing XRD measurements. A.T. also thanks the MICINN for Ramón y Cajal program (RYC-2010-05592). Finally, this work is dedicated to the memory of Prof. Iñaki Mondragon.

REFERENCES

(1) Decher, G. *Science* **1997**, *277*, 1232−1237.
(2) Yapei, W.; Han, P.; Wu, G.; Xu, H.; Wang, Z.; Zhang, X. *Langmuir* **2010**, *26*, 9736−9741.
(3) Hammond, P. T. *Adv. Mater.* **2004**, *16*, 1271−1293.
(4) Ferreira, Q.; Ribeiro, P. A.; Oliveira, O. N., Jr.; Raposo, M. *Appl. Mater. Interfaces* **2012**, *4*, 1470−1477.
(5) Serizawa, T.; Yamaguchi, M.; Akashi, M. *Biomacromolecules* **2002**, *3*, 724−731.
(6) Jiang, B.; Barnett, J. B.; Li, B. *Nanotechnol. Sci. Appl.* **2009**, *2*, 21−27.
(7) Rinaudo, M. *Prog. Polym. Sci.* **2006**, *31*, 603−632.
(8) Camilo, C. S.; dos Santos, D. S., Jr.; Rodrigues, J. J., Jr.; Vega, M. L.; Campana Filho, S. P.; Oliveira, O. N., Jr.; Mendonça, C. R. *Biomacromolecules* **2003**, *4*, 1583−1588.
(9) Muzzarelli, R. A. A.; Boudrant, J.; Meyer, D.; Manno, N.; DeMarchis, M.; Paoletti, M. G. *Carbohydr. Polym.* **2012**, *87*, 995−1012.
(10) Ravi Kumar, M. N. V. *React. Funct. Polym.* **2000**, *46*, 1−27.
(11) Serizawa, T.; Yamaguchi, M.; Akashi, M. *Biomacromolecules* **2002**, *3*, 724−731.
(12) Thierry, B.; Kujawa, P.; Tkaczyk, C.; Winnik, F. M.; Bilodeau, L.; Tabrizian, M. *J. Am. Chem. Soc.* **2005**, *127*, 1626−1627.
(13) Ahmad, N. M.; Saqib, M.; Barrett, C. J. *J. Macromol. Sci., Part A: Pure Appl. Chem.* **2010**, *47*, 571−579.
(14) Yager, K. G.; Barrett, C. J. *J. Photochem. Photobiol. A: Chem.* **2006**, *182*, 250−261.
(15) Kumar, S. K.; Hong, J.-D. *Langmuir* **2008**, *24*, 4190−4193.
(16) Natansohn, A.; Rochon, P. *Chem. Rev.* **2002**, *102*, 4139−4175.
(17) Delaire, J. A.; Nakatani, K. *Chem. Rev.* **2000**, *100*, 1817−1846.
(18) Xie, S.; Natansohn, A.; Rochon, P. *Chem. Mater.* **1993**, *5*, 403−411.
(19) Todorov, T.; Nicolova, L.; Tomova, N. *Appl. Opt.* **1984**, *23*, 4309−4312.
(20) Kim, D. Y.; Tripathy, S. K.; Li, L.; Kumar, J. *Appl. Phys. Lett.* **1995**, *66*, 1166−1168.
(21) Rochon, P.; Batalla, E.; Natansohn, A. *Appl. Phys. Lett.* **1995**, *66*, 136−138.
(22) Ikeda, T.; Mamiya, J.; Yu, Y. L. *Angew. Chem., Int. Ed.* **2007**, *46*, 506−528.
(23) Yu, Y. L.; Nakano, M.; Ikeda, T. *Nature* **2003**, *425*, 145−145.
(24) Li, M. H.; Keller, P.; Li, B.; Wang, X. G.; Brunet, M. *Adv. Mater.* **2003**, *15*, 569−572.
(25) Lim, H. S.; Han, J. T.; Kwak, D.; Jin, M.; Cho, K. *J. Am. Chem. Soc.* **2006**, *128*, 14458−14459.
(26) Lim, H. S.; Lee, W. H.; Lee, S. G.; Lee, D.; Jeon, S.; Cho, K. *Chem. Commun.* **2010**, *46*, 4336−4338.
(27) Goulet-Hanssens, A.; Sun, K. L. W.; Kennedy, T. E.; Barrett, C. J. *Biomacromolecules* **2012**, *13*, 2958−2963.
(28) Shi, X.; Shen, M.; Moehwald, H. *Prog. Polym. Sci.* **2004**, *29*, 987−1019.
(29) Arys, X.; Laschewsky, A.; Jonas, A. M. *Macromolecules* **2001**, *34*, 3318−3330.
(30) Shiratori, S. S.; Rubner, M. F. *Macromolecules* **2000**, *33*, 4213−4219.
(31) Yoo, D.; Shiratori, S. S.; Rubner, M. F. *Macromolecules* **1998**, *31*, 4309−4318.
(32) Decher, G.; Schmitt, J. *Prog. Colloid Polym. Sci.* **1992**, *89*, 160−164.
(33) Cunha, A. G.; Fernandes, S. C. M.; Freire, C. S. R.; Silvestre, A. J. D.; Pascoal Neto, C.; Gandini, A. *Biomacromolecules* **2008**, *9*, 610−614.
(34) Fernández, R.; Mondragon, I.; Oyanguren, P. A.; Galante, M. J. *React. Funct. Polym.* **2008**, *68*, 70−76.
(35) dos Santos, D. S., Jr.; Bassi, A.; Rodrigues, J. J., Jr.; Misoguti, L.; Oliveira, O. N., Jr.; Mendonça, C. R. *Biomacromolecules* **2003**, *4*, 1502−1505.
(36) dos Santos, D. S., Jr.; Bassi, A.; Misoguti, L.; Ginani, M. F.; Oliveira, O. N., Jr.; Mendonça, C. R. *Macromol. Rapid Commun.* **2002**, *23*, 975−977.
(37) Sailer, M.; Barrett, C. J. *Macromolecules* **2012**, *45*, 5704−5711 and references therein..
(38) Mehrotra, S.; Lynam, D.; Maloney, R.; Pawelec, K. M.; Tuszynski, M. H.; Lee, I.; Chan, C.; Sakamoto, J. *Adv. Funct. Mater.* **2010**, *20*, 247−258.
(39) Engler, A.; Bacakova, L.; Newman, C.; Hategan, A.; Griffin, M.; Discher, D. *Biophys. J.* **2004**, *86*, 617−628.
(40) Young, T. J.; Monclus, M. A.; Burnett, T. L.; Broughton, W. R.; Ogin, S. L.; Smith, P. A. *Meas. Sci. Technol.* **2011**, *22*, 125703−125709.
(41) Luo, H.; Shen, Q.; Ye, F.; Cheng, Y.-F.; Mezgebe, M.; Qin, R.-J. *Mater. Sci. Eng., C* **2012**, *32*, 2001−2006.
(42) Fery, A.; Schöler, B.; Cassagneau, T.; Caruso, F. *Langmuir* **2001**, *17*, 3779−3783.
(43) Ferreira, Q.; Ribeiro, P. A.; Raposo, M. J. *Appl. Phys.* **2013**, *113*, 243508(1)−243508(7).
(44) Mermut, O.; Lefebvre, J.; Gray, D. G.; Barrett, C. J. *Macromolecules* **2003**, *36*, 8819−8824.
(45) Song, O. K.; Wang, C. H.; Pauley, M. A. *Macromolecules* **1997**, *30*, 6913−6919.
(46) Fernández, R.; Ramos, J. A.; Espósito, L.; Tercjak, A.; Mondragon, I. *Macromolecules* **2011**, *44*, 9738−9746.
(47) Natansohn, A.; Rochon, P.; Gosselin, J.; Xie, S. *Macromolecules* **1992**, *25*, 2268−2273.
(48) Zucolotto, V.; Mendonça, C. R.; dos Santos, D. S., Jr.; Balogh, D. T.; Zilio, S. C.; Oliveira, O. N., Jr.; Constantino, C. J. L.; Aroca, R. F. *Polymer* **2002**, *43*, 4645−4650.